



Published in final edited form as:

*J Comp Neurol.* 2008 May 20; 508(3): 473–486. doi:10.1002/cne.21686.

## Modulation of Dendritic Spine Remodeling in the Motor Cortex Following Spinal Cord Injury:

### Effects of Environmental Enrichment and Combinatorial Treatment with Transplants and Neurotrophin-3

BYUNG G. KIM<sup>1,2</sup>, HAI-NING DAI<sup>1</sup>, MARIETTA MCATEE<sup>1</sup>, and BARBARA S. BREGMAN<sup>1,\*</sup>

<sup>1</sup>Department of Neuroscience, Georgetown University Medical Center, Washington, DC 20007

<sup>2</sup>Brain Disease Research Center, Department of Neurology, Ajou University School of Medicine, Suwon 443-721, Republic of Korea

#### Abstract

Incomplete spinal cord injury (SCI) elicits structural plasticity of the spared motor system, including the motor cortex, which may underlie some of the spontaneous recovery of motor function seen after injury. Promoting structural plasticity may become an important component of future strategies to improve functional outcomes. We have recently observed dynamic changes in the density and morphology of dendritic spines in the motor cortex following SCI. The present study sought to test whether SCI-induced changes in spine density and morphology could be modulated by potential strategies to enhance functional recovery. We examined the effects of enriched environment, transplants, and neurotrophin-3 on the plasticity of synaptic structures in the motor cortex following SCI. Housing rats in an enriched environment increased spine density in the motor cortex regardless of injury. SCI led to a more slender and elongated spine morphology. Enriched housing mitigated the SCI-induced morphological alterations, suggesting that the environmental modification facilitates maturation of synaptic structures. Transplantation of embryonic spinal cord tissue and delivery of neurotrophin-3 at the injury site further increased spine density when combined with enriched housing. This combinatorial treatment completely abolished the injury-induced changes, restoring a preinjury pattern of spine morphology. These results demonstrated that remodeling of dendritic spines in the motor cortex after SCI can be modulated by enriched housing, and the combinatorial treatment with embryonic transplants and neurotrophin-3 can potentiate the effects of enriched housing. We suggest that synaptic remodeling processes in the motor cortex can be targeted for an intervention to enhance functional recovery after SCI.

#### Keywords

spinal cord injury; dendritic spine; motor cortex; enriched environment; transplants; neurotrophin-3

---

Although traumatic injuries to the spinal cord often lead to a severe and permanent loss of motor function, patients suffering from incomplete spinal cord injury (SCI) show some evidence of spontaneous recovery (Burns et al., 1997; Marino et al., 1999). Because severed axons do not spontaneously regenerate, this functional recovery is probably mediated by

---

\*Correspondence to: Dr. Barbara S. Bregman, Department of Neuroscience, NRB Rm EP-04, Georgetown University Medical Center, 3970 Reservoir Rd. NW, Washington, DC 20007. E-mail: bregmanb@georgetown.edu

This article includes Supplementary Material available via the Internet at <http://www.interscience.wiley.com/jpages/0021-9967/suppmat>.

reorganization of spared motor system. The compensatory plasticity occurs at multiple levels of the neuraxis all the way from the spinal pattern generators below the lesion to the cortical motor centers in the brain (Raineteau and Schwab, 2001). Interventions aimed at promoting the extent of plasticity hold potential to enhance functional recovery after SCI (Blight, 2004; Hagg, 2006).

Synaptic structures, especially postsynaptic dendritic spines, are critical substrates for long-term changes in neural connections (Segal, 2005). Many different experimental or behavioral conditions are accompanied by various alterations in spine density and morphology (Yuste and Bonhoeffer, 2001; Hayashi and Majewska, 2005). Especially, changes in morphological pattern of dendritic spines have drawn a lot of interest, because spine morphology is a very critical determinant of its function (Yuste et al., 2000; Kasai et al., 2003). For example, slender spines with long necks are associated with higher electrical resistance (Araya et al., 2006), and longer spines are generally considered to be more immature (Portera-Cailliau et al., 2003). Elongated spines are often found in the brains of mentally retarded subjects (Purpura, 1975; Comery et al., 1997; Nimchinsky et al., 2001). In addition, changes in spine head size are associated with long-term changes in the efficiency of synaptic transmission (Matsuzaki et al., 2004).

Our previous study revealed dynamic remodeling of the dendritic spine structures in the motor cortex after SCI (Kim et al., 2006). The structural remodeling involved time-dependent alteration in spine density and marked changes in spine morphology. These findings suggested that the remodeling of spine structures underlies plasticity of the cortical connectivity after spinal injury, which has been demonstrated in various species, including humans (McKinley et al., 1987; Topka et al., 1991; Jain et al., 1997). We envision that, if manipulating the nature and/or extent of injury-induced spine remodeling is feasible, then structural plasticity at synapses could be utilized as a therapeutic target after SCI. The present study was designed to test whether axotomy-induced changes in spine density and morphology could be modulated by potential strategies to improve functional outcomes after SCI.

Enriched housing improves functional outcomes after various CNS injuries, including spinal cord trauma (Ohlsson and Johansson, 1995; Lankhorst et al., 2001; Koopmans et al., 2006), and exerts significant influence on synaptic structures (Globus et al., 1973). Therefore, we sought to determine whether housing animals under enriched conditions after SCI can affect the lesion-induced spine remodeling in the motor cortex. Future therapies for SCI that can be translated into clinics will certainly be a combination of neurorehabilitative measures and various local repair strategies (Dobkin and Havton, 2004; Dobrossy and Dunnett, 2005). One of the well-characterized repair strategies is transplantation of embryonic spinal cord tissue (Bregman et al., 1993; Anderson et al., 1995; Miya et al., 1997). We have demonstrated that embryonic transplants, especially with neurotrophin administration, support regeneration of severed axons and enhance recovery of motor function (Coumans et al., 2001; Lynskey et al., 2006). This treatment also promoted sprouting of the corticofugal axons in the spinal cord as well as at the brainstem level (Iarikov et al., 2007), suggesting that transplants and neurotrophins might have the capacity to modulate plasticity of the entire motor system. In this study, we also tested whether embryonic transplants and neurotrophin-3 (NT-3) in combination with enriched housing produce additive effects on spine structures in the motor cortex following SCI.

## MATERIALS AND METHODS

### Animals and spinal lesion

Adult female Sprague Dawley rats (200–250 g; Zivic Inc., Zelienople, PA) were used in this study. They were housed in the Georgetown University Division of Comparative Medicine

Facility, and all protocols were approved by the Georgetown University Animal Care and Use Committee. Animals received a right overhemisection injury at the C4 level. This injury removes the right hemicord plus the dorsal columns bilaterally. Cervical-level SCI will have more corticospinal neurons axotomized than the injury at thoracic level. It thus might also be advantageous to induce more vigorous cell body responses because of the proximity to corticospinal neurons (Fernandes et al., 1999). We use overhemisection rather than hemisection as a result of the technical difficulties posed in cutting a unilateral dorsal column without damaging the adjacent contralateral dorsal column. Detailed surgical procedures have been described elsewhere (Kim et al., 2006). This model has been well characterized in terms of the anatomical extent of injury and the pattern of behavioral recovery (Diener and Bregman, 1998a,b; Nikulina et al., 2004; Lynskey et al., 2006). Rats in the sham groups received only laminectomy, after which the incised muscles and skins were sutured in layer.

### Transplantation and administration of NT-3

After an overhemisection lesion, a subset of animals underwent transplantation of embryonic spinal cord tissues. During resection of host spinal cord, another experimenter collected fresh spinal cord tissue from E14 fetuses for transplantation. Details of transplants preparation have been previously described (Bregman and McAtee, 1993). Briefly, timed-pregnant rats were obtained at day 14 gestation. Sterile procedures were used to obtain the embryos for dissection. The fetuses were removed individually as needed and maintained in sterile culture medium (Dulbecco's modified Eagle's medium; Invitrogen Life Sciences, Grand Island, NY). The spinal cord was gently removed and stripped of dura and dorsal root ganglia. One- to three-millimeter segments of the cord were prepared for transplantation. After bleeding had completely stopped, transplants were gently placed into the overhemisection injury site. After transplantation, saline-soaked gelfoam was placed on top of transplants.

We used NT-3 in this study because our previous work showed that NT-3 effectively enhanced behavioral recovery and anatomical plasticity of the corticospinal tracts (Lynskey et al., 2006; Iarikov et al., 2007). Details of the procedures to deliver neurotrophins locally have been previously described (Coumans et al., 2001). After transplantation, gelfoam soaked with human recombinant NT-3 (1 mg/ml, diluted in saline; a generous gift from Regeneron Pharmaceuticals, Tarrytown, NY), instead of saline, was placed over the lesion and transplanted tissue. Osmotic minipumps (Alzet model 2002; Durect Corp, Cupertino, CA) filled with the amount of NT-3 sufficient for long-term 14-day delivery were prepared and placed subcutaneously on the right side dorsal and medial to the scapula. Minipump catheters were tunneled under the paraspinal muscles to deliver NT-3 over the lesion site. Minipumps were secured in place by a single suture at the proximal end of the catheter, and the muscle and skin were closed. The osmotic minipumps delivered NT-3 (1 mg/ml) at a rate of 0.5  $\mu$ l/hour continuously for 14 days.

### Enriched housing

The enriched housing cages used in this study measured 90  $\times$  60  $\times$  60 cm and housed five to seven animals together at the same time. In contrast, each standard cage measured 25  $\times$  46  $\times$  21 cm. The enriched housing is not only bigger than a standard cage but also contains a shelf, running wheel, hollow tubes, ramps, obstacles, balls, and toys (i.e., enhancement items) to encourage motor activity and to provide increased sensory feedback. The walls of the enriched cage are made of transparent plexiglas so that experimenters can easily watch animals from outside.

After surgery, all rats were initially placed into standard cages for 48 hours to facilitate postoperative recovery. After 48 hours, a subset of animals from each sham and injury group was transferred to enriched housing. Injured rats received food and water on the same side of

the cage during the first week to facilitate recovery. After that, food and water were placed on opposite sides of the enriched cage to promote locomotor activity. The increased size of the cage and number of animals in each cage encourage general activity and social interaction. The rats in enriched cages were transferred twice per week to newly cleaned and autoclaved cages. The enrichment items were rearranged at each transfer to provide maximum exposure to different stimuli.

### **Slice preparation and DiI labeling procedure**

To visualize dendritic spines in the motor cortex, fluorescently labeled neuronal processes were imaged by confocal microscopy. Compared with Golgi staining, this method allows more sensitive detection of spines and more accurate measurement of morphology. In addition, a much larger number of samples can be processed in a reasonable amount of time compared with electron microscopic analysis. For confocal microscopic imaging, fixed cortical slices were prepared. We did not consider *in vivo* live imaging because technical limitations of this method do not allow imaging of the deep layer that contains neurons directly axotomized by the spinal lesion. Dendritic processes were labeled with the fluorescent dye DiI by direct application. We previously reported that lowering the concentration of fixative improved filling and diffusion of the fluorescent dye through the neuronal membrane (Kim et al., 2007). All animals were sacrificed 4 weeks after spinal lesion or sham operation and fixed with 1.5% paraformaldehyde in 0.1 M phosphate buffer. The brains were postfixed in the same fixative for 1 hour and then transferred to and kept in cold phosphate-buffered saline (PBS; pH 7.4) until they were sliced. On the same day, brains were divided into two hemispheres, and only the left hemispheres were coronally sectioned into 200- $\mu$ m slices with a vibratome (model Vibratome 1000 classic; Technical Products Int'l. Inc., O'Fallon, MO). Slices containing the forelimb motor cortex were collected in PBS. The rostrocaudal extent of the forelimb motor cortex was determined according to a previous mapping study (Donoghue and Wise, 1982). Slices containing forelimb motor cortex are positioned between +1.7 mm and +0.4 mm from bregma. Typically, we began collecting slices when the striatum could be clearly identified, and the first sections of several serially sectioned slices (in a rostrocaudal direction) were used for DiI labeling.

The detailed procedure for DiI labeling was described previously (Kim et al., 2007). Briefly, fine crystals of solid DiI (1,1'-dioctadecyl-3,3',3'-tetramethylindocarbocyanine perchlorate; catalogue No. D-282; Molecular Probes, Eugene, OR) were applied to the slices (left hemisphere) using a glass micropipette with a sharp and elongated tip. We delivered DiI crystals separately onto superficial layers (2/3) and deep layers (5/6) in the motor cortex. The lateral border of the forelimb motor cortex could be identified by a transition of luminance pattern from the granule cell layer in the S1 area to the agranular cortex under illumination. DiI crystals on the slices were allowed to diffuse for 4–12 hours in PBS at room temperature. Slices were then fixed again with 4% paraformaldehyde for 30 minutes, washed in PBS three times each for 5 minutes, and stored in cold PBS. Slices were mounted on glass slides with Mowiol, a glycerol-based mounting medium (Calbiochem, La Jolla, CA), and coverslipped. All images were taken within 7 days after coverslipping. Before images were taken, all slides were assigned randomized codes to ensure analysis blind to experimental conditions.

### **Laser confocal microscopic imaging and image analysis**

Labeled dendritic processes in the left motor cortex were imaged using a Zeiss 510 Meta confocal laser scanning microscope (LSM 510 META). Basal dendritic segments that were well separated from neighboring neural processes were randomly sampled in both the superficial and the deep layers of the forelimb motor cortex. For basal dendrites, dendritic segments that run tangentially or toward the white matter were imaged. Each dendritic segment we imaged belonged to a different neuron. All images were taken using the Plan-Apochromat

X63 oil-immersion lens (N/A 1.4). All imaging parameters were the same as described previously (Kim et al., 2007). Detector settings were varied to maximize dynamic range for spine images. We used  $2,048 \times 2,048$  pixels for frame size, without zooming. Serial stack images with step size ranging from 0.4 to 0.6  $\mu\text{m}$  were collected.

MetaMorph software (Universal Imaging Corporation, Downingtown, PA) was used for image analysis. A series of stack images for each selected dendrite was imported into MetaMorph, which then generated a 3D projection image. Both a series of stack images and a 3D projection image were used in a complimentary manner to increase the sensitivity of spine detection. Spine number was divided by the length of dendritic segment to generate dendritic spine density expressed as number per micrometer. It is worth noting that it was technically difficult to count the number of spines accurately in the segments with a very high spine density. For example, if spine density is higher than 2.5 spines/ $\mu\text{m}$ , the spines were too crowded to separate individual ones even with the complimentary image analysis (see Fig. 5B). All dendritic spines counted for density analysis were used for the analysis of morphology. The head diameter was measured using the “Single line” tool, and spine length was measured using the “Traced line” tool in the software. Head diameter was defined as the length of longest straight line through the spine head orthogonal to the neck of spine. Spine length was defined as the distance from the outer edge of the dendritic shaft and to the tip of the spine. Filopodium-like dendritic protrusions were defined as being longer than 5  $\mu\text{m}$  in length, which is a relatively conservative criterion compared with a previous study (Lendvai et al., 2000). We took basal dendritic segments at least 30  $\mu\text{m}$  away from the cell body, because we found that spine density is consistently lower at the dendritic segment very close to the cell body. For production of photomicrographs, image files were imported into PhotoShop 7 (Adobe, San Jose, CA) and post-processed to generate multipanel figures. Brightness and contrast were not manipulated at this stage.

### Statistical analysis

All numerical data are presented as mean  $\pm$  SEM. Statistical analysis was performed with SPSS version 12.0 (SPSS, Chicago, IL) or GraphPad Prism version 4.0 (GraphPad, San Diego, CA). Two-way ANOVA was performed to determine the effect of either housing factor (standard vs. enriched housing) or injury factor (sham vs. injury) independently or their possible interaction on spine density and morphology. If any of these factors turned out to be significant, post hoc Bonferroni's test was performed to compare means between groups. Distributions of morphological variables (head diameter, spine length, and aspect ratio) did not conform to the Gaussian, normal distribution (by one-sample Kolmogorov-Smirnov test). To perform parametric two-way ANOVA for the dependent variables that do not conform to a normal distribution, we used a log transformation for the analysis of head diameter, spine length, and aspect ratio (Keene, 1995). In log transformation, natural logs of the values for dependent variable were used instead of the original raw values. The two-sample Kolmogorov-Smirnov test was used to compare the patterns of cumulative or relative frequency plots in the histogram of individual values for spine density, head diameter, and length between standard and enriched housing groups. Comparison of group means in spine density was performed with one-way ANOVA followed by post hoc Bonferroni's test. Because the morphology variables do not conform to Gaussian distribution, the nonparametric Kruskal-Wallis test was used to determine significance of group effect, and the Mann-Whitney U test was used for comparison between each group to analyze the morphology variables. Spine densities obtained from different dendritic segments (thus different neurons in this study) or morphology data from different dendritic spines were highly variable even in one animal. We found that between-neuron variability or between-spine variability could explain most of the total group variability (measured as coefficients of variation) of density or morphology data, respectively. To take into account intrinsic variability between dendritic segments or between spines, we treated

each dendritic segment for density analysis or each spine for morphology analysis as an independent observation.

## RESULTS

### Influence of enriched housing on dendritic spine structures in the motor cortex following SCI

To examine whether environmental modification modulates the density and morphology of dendritic spines in the motor cortex, subsets of rats with sham operation (laminectomy only) or a cervical overhemisection injury at C4 level were housed in large cages enriched with various items to enhance motor activity and were compared with those housed in standard cages. In total, four experimental groups were generated: 1) sham controls in standard housing (SS group,  $N = 5$ ), 2) sham controls in enriched housing (ES group,  $N = 6$ ), 3) rats with spinal injury in standard housing (SHx group,  $N = 6$ ), and 4) rats with spinal injury in enriched housing (EHx group,  $N = 6$ ). All rats survived for 28 days, after which they were killed for visualization of dendritic spines in the left forelimb motor cortex. Detailed numerical values are presented in Tables 1 and 2 (for the superficial and deep layers, respectively).

**Spine density**—Enriched housing increased spine density in the superficial layer in uninjured animals (SS and ES groups; Fig. 1A), resulting in a rightward shift of density distribution in the cumulative frequency histogram (Fig. 1B). The mean spine density was increased by  $11.2\% \pm 2.9\%$  (Fig. 1C). The extent of increase by enriched housing is comparable to that in the original work reporting a 9.7% increase in spine density of the visual cortex with enriched environment (Globus et al., 1973). Enriched housing increased spine density also in the animals with cervical overhemisection injury. Spine density distribution of the EHx group significantly shifted to the right compared with that of the SHx group (Kolmogorov-Sminorv test,  $P < 0.05$ ), and the mean spine density was increased by  $16.8\% \pm 3.5\%$  (Fig. 1B,C). Two-way ANOVA revealed significant housing effect ( $P < 0.001$ ), whereas the injury factor was not statistically significant. Post hoc Bonferroni's test revealed a significant housing effect in both sham and injured animals (Fig. 1C). The interaction between housing and injury factors was not significant, suggesting that the effect of enriched housing on spine density does not depend on injury condition. Spine density in the deep layer dendritic segments was also increased by an exposure to enriched housing (Fig. 1D,E). Density distribution in the cumulative frequency histogram tended to shift to the right in both sham (SS vs. ES) and injured (SHx vs. EHx) animals (Fig. 1D). The extent of increase in the mean spine density with enriched housing was  $12.1\% \pm 3.7\%$  in sham operates (SS vs. ES) and  $9.9\% \pm 2.9\%$  in injured groups (SHx vs. EHx; Fig. 1E). Similarly to the case in the superficial layer, housing condition significantly affected spine density ( $P < 0.01$ ), although the injury factor was not significant. The mean difference was significant only between sham operates by post hoc Bonferroni's test, not between SHx and EHx groups (Fig. 1E). Interaction between housing and injury factors was not statistically significant. Taken together, analysis of spine density showed that enriched housing increases spine density in both sham and injured animals. The housing effect was not dependent on the injury condition. The effect of enriched housing for injured rats seems to be more pronounced in the superficial than in the deep layer.

**Spine head diameter**—Spine head diameter was measured from the same set of dendritic segments used for the density analysis. In total, 7,547 and 6,485 spines were analyzed in the superficial and deep layers, respectively (Tables 1, 2). In the superficial layer, distributions of head diameter in the frequency histogram in sham operates (SS vs. ES) were almost identical (Fig. 2A). Head diameter distribution of the EHx group was also similar to that of the SHx group. The mean head diameter was slightly smaller in both SHx and EHx groups compared with sham control animals (by 1.8% in SS vs. SHx, by 1.6% in ES vs. EHx; Fig. 2B). The

housing effect was not significant by two-way ANOVA, but the injury effect produced significant differences ( $P < 0.01$ ). Interaction between the two factors was not significant. In the deep layer, spinal injury led to an increase in the proportion of larger spine head, resulting in a significant shift of the diameter distribution to the right in the frequency histogram (Fig. 2C; Kolmogorov-Sminorv test for SS vs. SHx group,  $P < 0.01$ ). Enriched housing decreased the proportion of larger spine head, and it further shifted the distribution of head diameter of the EHx group even to the left compared with sham operation. As a result, the difference between the distributions of head diameter in SHx and EHx groups was highly significant (Kolmogorov-Sminorv test,  $P < 0.001$ ). Mean head diameter of the SHx group was 2.2% greater than that of SS group (Fig. 2D;  $P < 0.01$  by Mann-Whitney U test). In contrast, head diameter in injured rats housed in the enriched condition (EHx) was even smaller than that in the SS group, suggesting that enriched housing completely abolishes the injury-induced increases in head diameter. Housing effect on head diameter was highly significant by two-way ANOVA ( $P < 0.001$ ). Interaction between the housing and the injury factors was also highly significant ( $P < 0.001$ ), suggesting that enriched housing exerts a robust effect on head diameter for injured animals in the deep layer, but not for sham-operated animals.

**Spine length**—Spine length was measured from the same population of dendritic spines as for the analysis of head diameter. Housing in the enriched environment did not apparently change spine length distributions in sham-operated animals in either superficial or deep layers (Fig. 3A,C; SS vs. ES). Spinal injury significantly shifted the distribution of spine length to the right in the frequency histogram (Fig. 3A,C; SS vs. SH,  $P < 0.001$  by Kolmogorov-Sminorv test in both layers). The extent of spine elongation after spinal injury was reduced by enriched housing, resulting in a significant difference in the distributions of spine length in SHx vs. EHx groups (Kolmogorov-Sminorv test,  $P < 0.001$  in both layers). Mean spine length in the EHx group was still greater than that in SS group, but much smaller than that in SHx group (Fig. 3B). There was a significant housing ( $P < 0.05$ ) and injury effect ( $P < 0.001$ ) on spine length, and the interaction between the two factors was also highly significant ( $P < 0.001$ ) in the superficial layer (Fig. 3B). In the deep layer, both the housing and the injury factors were significant, and the interaction between the two was also significant (Fig. 3D; housing,  $P < 0.001$ ; injury,  $P < 0.001$ ; housing  $\times$  injury,  $P < 0.001$ ). Post hoc Bonferroni's test revealed a significant housing effect only in injured animals and significant injury effect in both housing conditions in both layers (Fig. 3B,D). Taken together, these results from the analysis of spine length suggested that an injury at the spinal level leads to an elongation of dendritic spines by 28 days in the motor cortex and that enriched housing decreases spine length in injured rats. In contrast, spine length is not significantly affected in sham controls by enriched housing.

Because spine length is developmentally regulated, longer spines are generally considered less mature than shorter ones (Portera-Cailliau et al., 2003). In this regard, a decrease in mean spine length by an exposure to enriched housing may suggest that the environmental modification facilitates maturation of synaptic structures that are being remodeled after SCI. To examine this possibility, we analyzed the frequency of filopodium-like long dendritic protrusions ( $>5 \mu\text{m}$ ). Filopodial dendritic protrusions are observed mostly during development (Miller and Peters, 1981), when they participate in initial contacts to presynaptic terminals (Fiala et al., 1998). All the spines from both the superficial and the deep layers were pooled together for this analysis, because there were very few filopodium-like long protrusions in sham-operated rats. We found 14 filopodium-like protrusions among 3,038 spines (0.46%) in sham-operated rats in standard cages (SS group; Fig. 3E). The frequency dropped to 0.15% (6 of 3,906) in the ES group. Spinal injury greatly increased the frequency of filopodium-like protrusions (SHx, 1.22%, 50 of 4,087). Injured rats in enriched housing (EHx group) had a higher frequency than sham-operated groups, but, compared with SHx group, the frequency dropped by about half (0.73%, 22 of 3,001 spines).  $\chi^2$  Analysis revealed a significant difference in the frequency of filopodium-like long dendritic protrusions between SHx and EHx groups ( $\chi^2 = 4.137$ ,  $P < 0.05$ )

as well as SS and ES groups ( $\chi^2 = 5.616$ ,  $P < 0.05$ ). To control for differences in the spine density between groups, the number of filopodium-like protrusions per 100  $\mu\text{m}$  dendrites, which is a density of filopodium-like protrusions, was separately obtained (Fig. 3F). The density of filopodium-like protrusions showed a similar trend (SS, 0.88; ES, 0.32; SHx, 2.13; EHx, 1.45). These data showed that an exposure to enriched housing reduced the frequency of filopodium-like dendritic protrusions, suggesting that the environmental modification may facilitate maturation of the synaptic connections in the motor cortex following SCI.

**Aspect ratio (AR)**—Morphology of dendritic spines significantly affects spine function (Hayashi and Majewska, 2005). Head size determines the amount of synaptic currents, and spine length controls the time window of calcium compartmentalization and filters membrane potentials into the spine heads (Yuste et al., 2000; Araya et al., 2006). A theoretical modeling study also indicates that the conductance ratio between the spine head and neck critically determines the spines' electrical behavior (Koch et al., 1992), suggesting that a relative ratio between spine length and head diameter in each spine, rather than absolute length or diameter, determines functional characteristics of the spine. We therefore divided spine length by head diameter to obtain an aspect ratio (AR) from each spine (Fig. 4A). A spine with lower AR will be shorter and fatter, and a spine with higher AR will be longer and thinner (Wallace and Bear, 2004). Higher AR may also indicate that a spine is longer or more slender even after adjusting for differences in head diameter.

In the superficial layer, AR in sham operated was not significantly changed by an exposure to enriched housing (ES group; Fig. 4B). Spinal injury led to an increase in AR compared with SS group. Housing rats in enriched housing after injury reduced AR, but the mean AR in EHx group was still higher than that in sham-operated animals (SS or ES group). Injury factor was highly significant in both housing conditions ( $P < 0.001$ ; Fig. 4B). Housing effect was also significant ( $P < 0.05$ ), but only between injured groups, by the post hoc Bonferroni's test (Fig. 4B). The interaction between injury and housing factors was significant ( $P < 0.01$ ), suggesting that enriched environment plays a modulatory role mostly for the dendritic spines that are being remodeled after spinal injury. Spinal injury also led to an increase in AR in the deep layer (Fig. 4C). Enriched housing tended to decrease AR in injured rats, but to a smaller extent than in the superficial layer. Injury effect was still highly significant in the deep layer in both housing conditions ( $P < 0.001$ ; Fig. 4C). Housing effect was marginally significant ( $P < 0.05$ ), but the post hoc Bonferroni's test did not show significant differences between either sham-operated or injured groups (Fig. 4C), suggesting that enriched housing alone was not sufficient to mitigate significantly injury-induced alteration in spine morphology in the deep layer even in the injured animals. Taken together, these data indicate that the morphology of dendritic spines in the motor cortex becomes more slender after axotomy of their output axons at the spinal cord. Enriched housing tended to mitigate the morphological alteration, but the effect of enriched housing was significant only in the superficial layer.

### **Effects of transplants and NT-3 in combination with enriched housing on spine density and morphology**

To examine whether transplantation of embryonic spinal cord and/or administration of NT-3 produced additive effects on spine remodeling in combination with enriched housing, we generated three more experimental groups: 1) rats with injury and transplantation in standard housing (STP group,  $N = 5$ ), 2) rats with injury and transplantation in enriched housing (ETP group,  $N = 5$ ), and 3) rats with injury and transplantation and NT-3 in enriched housing (ENT group,  $N = 5$ ). Spine density and morphology in these groups were compared with those in sham-operated animals housed in the standard condition (SS group) and the animals with spinal injury housed in standard or enriched conditions (SHx and EHx group, respectively).

Measurement variables and the data are summarized in Table 1 and 2 (for the superficial and deep layers, respectively).

**Spine density**—As shown in Figure 1, mean spine density in the superficial layer of SHx group in the forelimb motor cortex was lower than in the SS group, and housing injured rats in enriched condition (EHx group) markedly increased the mean spine density. Transplantation of embryonic spinal cord at the injury site (STP group) had a similar effect on spine density, increasing the mean spine density by  $16.7\% \pm 3.1\%$  (compared with SHx group; Fig. 5A). The extent of increase in spine density by combination of transplantation with enriched housing (ETP group) was comparable to that observed in either condition alone. Administration of NT-3 for the initial 2 weeks in addition to the above-described interventions (ENT group) resulted in the largest increase among all the groups (Fig. 5B). One-way ANOVA revealed a highly significant group effect ( $P < 0.001$ ). Post hoc Bonferroni's test showed that only the ENT group had significantly higher mean density compared with the animals without any intervention (SS group;  $P < 0.05$ ). The mean spine density of the injured animals with any of the interventions (EHx, STP, ETP, and ENT) was significantly higher than that of the injured animals without any intervention (SHx group;  $P < 0.05$  vs. EHx;  $P < 0.01$  vs. STP and ETP;  $P < 0.001$  vs. ENT). A possible additive effect of NT-3 administration was not evident, because there was no significant difference between ENT and any of EHX, STP, and ETP groups. However, some of the dendritic segments in ENT group were studded with too many spines to be isolated from each other (Fig. 5B, arrows; see Materials and Methods). Therefore, some of the NT-3 effects on spine density might not be uncovered as a result of difficulties in counting all the individual spines from the highly crowded segments.

Spine density in the deep layer was also increased by different combinations of interventions (Fig. 5C). The extent of difference, however, was not as robust as that observed in the superficial layer. Although the effect of transplantation on spine density was modest (STP and ETP groups), addition of NT-3 still showed the largest extent of increase (ENT group; Fig. 5D). There was no significant group effect on spine density in the deep layer ( $P = 0.07$ ). In summary, analyses of spine density showed that enriched housing and transplantation of embryonic spinal cord tissue at the injury site each or in combination tended to increase the density of dendritic spines. The increases were more robust in the superficial layer. Administration of NT-3 for the initial 2 weeks in addition to the other two interventions achieved the highest mean spine density in both layers, suggesting a possible additive effect of NT-3 on spine density.

**Spine morphology**—AR (length divided by diameter) accommodates both the length and the head diameter, so the functional properties of each spine may be inferred more properly from its AR rather than either length or diameter. Therefore, we focused on the changes in a morphological pattern as represented by AR. Detailed data on head diameter and spine length are presented in the supplementary information (Supplementary data and figure). As shown in Figure 4A, spinal injury dramatically increased the mean AR, and enriched housing alone reduced the extent of the injury-induced increase in AR. Transplantation alone also decreased AR to a similar extent (Fig. 6A). Combination of transplantation and enriched housing (ETP group) resulted in a further decrease, almost reaching the value of SS group. Addition of NT-3 (ENT group) decreased AR to an extent similar to that in the ETP group. Kruskal-Wallis test showed a significant group effect ( $P < 0.001$ ). Post hoc Mann-Whitney U test revealed significant differences between SHx and each of the other groups. The mean ARs in ETP and ENT groups were also significantly different from that in EHx group ( $P < 0.01$  and  $P < 0.001$ , respectively), suggesting a significant additive effect of transplantation with or without NT-3. The animals in ETP and ENT groups seemed to regain a normal pattern of spine morphology, because the mean ARs of the two groups were not significantly different from that of SS group.

The mean AR of the spines in the deep layer after spinal injury was also decreased by either enriched housing or transplantation alone, but to a modest extent compared with the superficial layer (Fig. 6B). Again, combination of transplantation and enriched housing (ETP group) decreased AR greater than either alone did. Addition of NT-3 (ENT group) further decreased AR and even resulted in lower mean AR than the preinjury value (in SS group). A significant group effect was revealed ( $P < 0.001$ ), and post hoc Mann-Whitney U test showed significant differences between SHx and each of the other groups. The differences between EHx and ETP or ENT were highly significant ( $P < 0.01$  and  $P < 0.001$ , respectively), and the mean ARs of the latter two groups were not different from the AR of the SS group. The difference between ETP and ENT groups was also significant ( $P < 0.05$ ), demonstrating a significant additive effect of NT-3. Taken together, these results indicate that, although enriched housing alone modestly, if at all, reduces the degree of slenderness of dendritic spines after injury, both transplantation and NT-3, when combined with enriched housing, can almost completely abolish spinal injury-induced morphological alterations and restore a preinjury morphological pattern.

## DISCUSSION

Our previous work showed that synaptic structures in the motor cortex undergo dynamic remodeling following SCI (Kim et al., 2006). The present study demonstrates that the spine remodeling is heavily affected by various interventions to improve functional outcomes after SCI. The effect was most striking on spine morphology; enriched housing tended to counteract injury-induced spine elongation. A combined application of transplants and NT-3 almost completely restored a preinjury pattern of morphology. Dynamic modulation of morphology of a large population of spines suggests that the overall functional properties in the motor cortical network are significantly altered by the interventions following SCI.

Enriched housing increased spine density in the motor cortex of both sham and injured animals. This suggests that enriched housing influences synaptogenic processes after injury in a way similar to the way it does in the intact brain (Globus et al., 1973; Moser et al., 1994). This was also true in the stroke model, in which enriched housing increased spine density in both sham and stroke groups (Johansson and Belichenko, 2002). Higher spine density suggests an increase in complexity of synaptic connections in a given network. The increase in complexity may in turn contribute to improved functional recovery by enriched environment after SCI (Lankhorst et al., 2001; Van Meeteren et al., 2003; Koopmans et al., 2006). Although enriched housing is supposed to exert neuroanatomical effects on the whole brain, housing rats after injury under enriched conditions may exert some unique effects on the motor cortex compared with other parts of the cortex or the intact brains. Spine density in the motor cortex decreases by 7 days after SCI and partially recovers by 28 days (Kim et al., 2006), suggesting an increase in the rate of new spine formation between these two time points. Enriched housing may accelerate the injury-induced synaptogenesis or stabilize newly generated synapses in the motor cortex.

In contrast to the well-established link between spine density and enriched housing, surprisingly little is known about whether spine morphology, which is a critical determinant of synaptic function (Yuste et al., 2000), is affected by enriched housing. By using confocal microscopy, the effects of enriched housing on spine morphology were analyzed quantitatively and systematically. Spinal injury elicited a dynamic alteration in morphology, especially length, at the 4 week time point. Although spine morphology was not changed in the sham group, an exposure to enriched housing after injury decreased the proportion of longer spines compared with injured rats in standard housing. This finding suggests two possibilities. 1) Newly added spines by enriched housing are shorter than an already-existing population of spines. 2) Initial length of new spines might have a similar distribution, but enriched housing shortens the length of the whole population of spines. According to the former possibility, the

number of filopodium-like long protrusions per fixed length of dendrites (density) should not be affected by enriched housing. The observation that the density, along with the proportion, of filopodium-like protrusions was reduced in the EHx group (Fig. 3F) favors the latter explanation. Several studies reported a similar spine shortening with electrical stimulation (Fifkova and Anderson, 1981) and changes in experiences (Coss and Globus, 1978; Coss et al., 1980; Brandon and Coss, 1982) in uninjured, naïve organisms. We observed significant environmental effects only in injured animals, suggesting that environmental modification has more pronounced effects on the spines that have already been evoked to undergo remodeling than naïve spines without any eliciting stimulus.

Because both the head size and the length of each spine are critically involved in determining its functional characteristics (Yuste et al., 2000), we obtained aspect ratio (AR; spine length divided by head diameter) from each spine as an index of the slenderness (Fig. 4A). A dramatic increase in AR indicates that dendritic spines in the motor cortex become more slender after SCI. More slender spines with long necks present higher electrical resistance to synaptic currents flowing from the spine head (Koch et al., 1992; Araya et al., 2006), resulting in a less efficient synaptic transmission. The spine neck can act as a barrier to diffusion of small molecules such as calcium ions (Svoboda et al., 1996), and the kinetics of postsynaptic calcium are highly dependent on spine morphology (Noguchi et al., 2005). An increase in slenderness of spines may result in a longer accumulation of calcium in spine heads, which in turn may lead to a stronger activation of the synaptic plasticity process. Thus, more slender morphology may indicate a heightened capacity for synaptic plasticity. Overall, an increase in AR of a large population of dendritic spines may indicate immaturity of synaptic connections (less efficient and more plastic) in the motor cortical network. An exposure to enriched housing tended to abolish the injury-induced increases in AR in the superficial layer, suggesting that enriched housing promotes maturation of synaptic connectivity. A recent study reported that rearing FMR1-knockout mice, a model for fragile X syndrome, in enriched housing resulted in more mature spine morphology (Restivo et al., 2005). Thus, enriched housing seems to promote maturation of spine morphology in various pathologic conditions in which immature spine morphology can be observed.

We found that combination of transplants and NT-3 with enriched housing achieved the highest spine density. Furthermore, the combinatorial approach potentiated the effects of enriched housing on AR, almost completely restoring a preinjury pattern of morphology. The additive effects of transplants and NT-3 suggest that the mechanism by which the interventions affect synaptic structures may differ from that of enriched housing. Unlike enriched housing, transplants and NT-3 are supposed to exert their effects locally at the injured spinal cord (C4). We have shown that the embryonic transplants at the injury site, especially with neurotrophic factors, provide strong trophic supports to the injured supraspinal motor neurons (Bregman et al., 1998). It is thus possible that the trophic effects could stimulate axotomized cortical neurons and other interconnected neurons in the circuit to undergo more potent remodeling process. NT-3, after it is retrogradely transported, may exert a direct influence on synaptic structures insofar as it plays an important role in synaptogenesis and maintenance of the synaptic structures (Martinez et al., 1998; Collin et al., 2001). Alternatively, NT-3, combined with transplants, may indirectly affect synaptic structures in the motor cortex. We have shown that transplants and NT-3 enhanced plasticity of the corticofugal fibers at the brainstem and spinal cord (Iarikov et al., 2007). The increases in sprouting of cortical projection fibers, which might be accompanied by increases in connections with appropriate targets, may further enhance reorganization of synaptic connectivity in the motor cortex. Together, our results suggest that the local repair strategy (transplants and NT-3) and enriched housing may act synergistically to produce more potent modulatory effects on synaptic structures. The results in this study may have important clinical implications, because future treatment for patients with SCI is likely to involve local repair strategies coupled to neurorehabilitative measures (such as enriched

housing) that can optimize the injury-induced plasticity (Dobkin and Havton, 2004; Dobrossy and Dunnett, 2005).

Neurons in the superficial layer are chiefly involved in corticocortical connections, whereas deep layer neurons send projection axons out of the cortex. It is possible, therefore, that neurons in different layers may respond differently to spinal injury (axotomy) and the interventions employed in this study. We consistently found that increases in spine density by enriched housing and transplants were more pronounced in the superficial than in the deep layer. It remains to be answered why generation or retraction of dendritic spines occurs more actively in the superficial than in the deep layer where axotomized neurons are located. It could be argued that the corticocortical connections in the superficial layer may play a more major role in the lesion-induced cortical plasticity. Morphology of dendritic spines as measured by AR responded to the environmental modification more sensitively also in the superficial layer (Fig. 4). In contrast, the additive effect of NT-3 on spine morphology was evident only in the deep layer (Fig. 6). Therefore, it is conceivable that the extent to which an intervention such as enriched housing and NT-3 modulates remodeling of spine morphology may vary depending on the layer to which dendritic spines belong. The layer-dependent differences have been reported in the plasticity of somatosensory cortex during development (Diamond et al., 1994).

To summarize, this study demonstrates that the nature and/or extent of spine remodeling can be manipulated by various interventional strategies such as enriched housing, transplants, and NT-3. The interventions, especially a combination of the three, increased the complexity of synaptic connectivity by adding more spines and promoted maturation of synaptic structures. This highlights an interesting possibility, that structural remodeling of dendritic spines in the motor cortex can be targeted for a future strategy to improve motor recovery following SCI. For example, if we can intervene in the synaptic remodeling process, aiming to promote new synapse formation and/or synaptic maturation, better functional outcomes could be expected. A more thorough understanding of the synaptic remodeling processes, as well as knowledge about the molecular mechanisms underlying the morphological plasticity of synaptic structures (Sheng and Kim, 2002), will be required to design a proper strategy to target the synaptic remodeling process.

## Supplementary Material

Refer to Web version on PubMed Central for supplementary material.

## ACKNOWLEDGMENTS

We thank Dr. Bogdan Stoica for technical advice on confocal microscopy and Dr. Stefano Vicini for valuable suggestions and comments. We also deeply appreciate discussions on statistical issues with Dr. Shibao Feng at the Biostatistics and Bioinformatics Shared Resource in Lombardi Cancer Center, Georgetown University Medical Center.

Grant sponsor: National Institutes of Health; Grant number: NS 27054; Grant number: NS 051656-01A1.

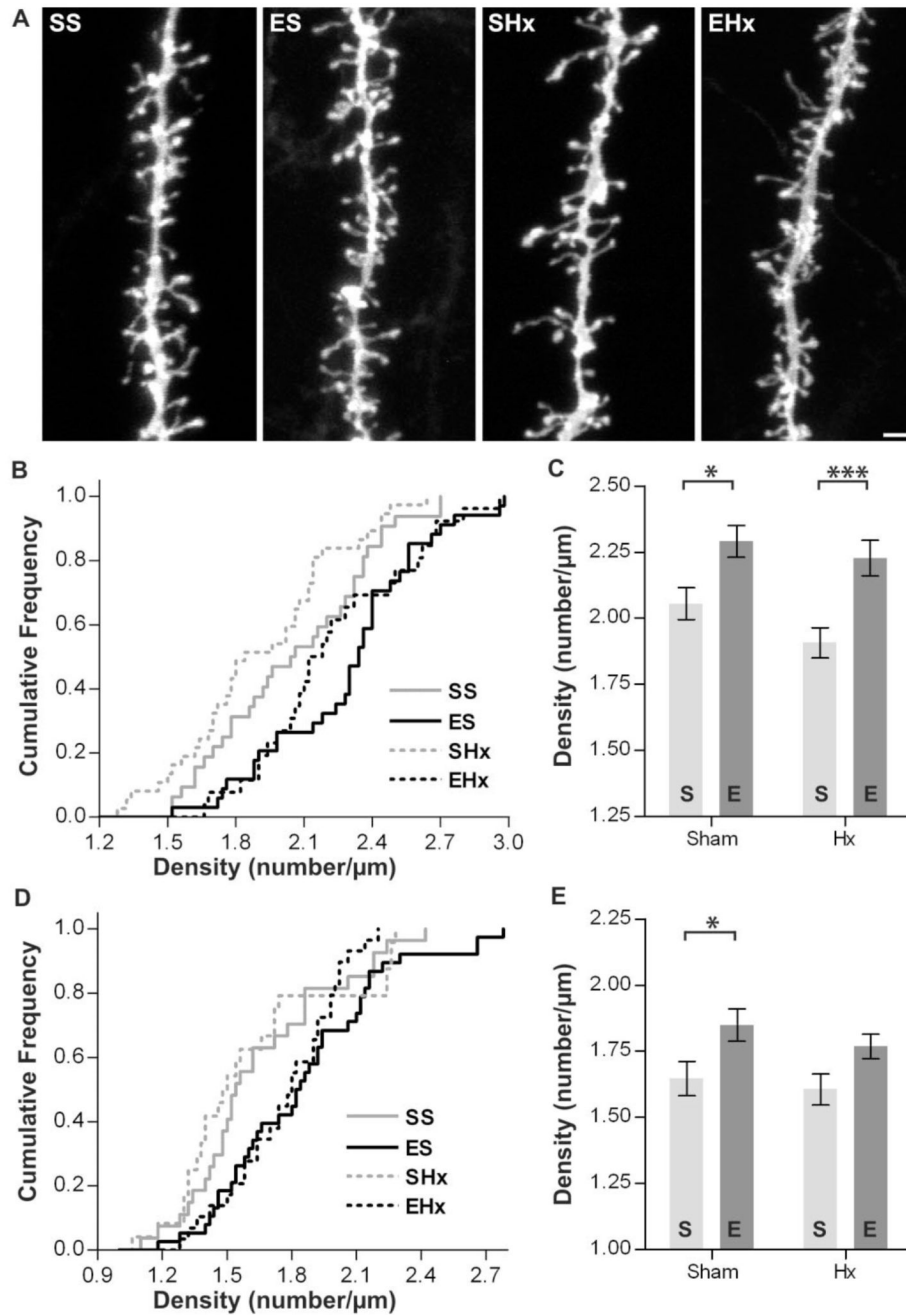
## LITERATURE CITED

- Anderson DK, Howland DR, Reier PJ. Fetal neural grafts and repair of the injured spinal cord. *Brain Pathol* 1995;5:451–457. [PubMed: 8974628]
- Araya R, Jiang J, Eisenthal KB, Yuste R. The spine neck filters membrane potentials. *Proc Natl Acad Sci U S A* 2006;103:17961–17966. [PubMed: 17093040]
- Blight AR. Just one word: plasticity. *Nat Neurosci* 2004;7:206–208. [PubMed: 14983180]
- Brandon JG, Coss RG. Rapid dendritic spine stem shortening during one-trial learning: the honeybee's first orientation flight. *Brain Res* 1982;252:51–61. [PubMed: 7172021]

- Bregman BS, Kunkel-Bagden E, Reier PJ, Dai HN, McAtee M, Gao D. Recovery of function after spinal cord injury: mechanisms underlying transplant-mediated recovery of function differ after spinal cord injury in newborn and adult rats. *Exp Neurol* 1993;123:3–16. [PubMed: 8405277]
- Bregman BS, Broude E, McAtee M, Kelley MS. Transplants and neurotrophic factors prevent atrophy of mature CNS neurons after spinal cord injury. *Exp Neurol* 1998;149:13–27. [PubMed: 9454611]
- Burns SP, Golding DG, Rolle WA Jr, Graziani V, Ditunno JF Jr. Recovery of ambulation in motor-incomplete tetraplegia. *Arch Phys Med Rehabil* 1997;78:1169–1172. [PubMed: 9365343]
- Collin C, Vicario-Abejon C, Rubio ME, Wenthold RJ, McKay RD, Segal M. Neurotrophins act at presynaptic terminals to activate synapses among cultured hippocampal neurons. *Eur J Neurosci* 2001;13:1273–1282. [PubMed: 11298787]
- Comery TA, Harris JB, Willems PJ, Oostra BA, Irwin SA, Weiler IJ, Greenough WT. Abnormal dendritic spines in fragile X knockout mice: maturation and pruning deficits. *Proc Natl Acad Sci U S A* 1997;94:5401–5404. [PubMed: 9144249]
- Coss RG, Globus A. Spine stems on tectal interneurons in jewel fish are shortened by social stimulation. *Science* 1978;200:787–790. [PubMed: 644322]
- Coss RG, Brandon JG, Globus A. Changes in morphology of dendritic spines on honeybee calycal interneurons associated with cumulative nursing and foraging experiences. *Brain Res* 1980;192:49–59. [PubMed: 7378790]
- Coumans JV, Lin TT, Dai HN, MacArthur L, McAtee M, Nash C, Bregman BS. Axonal regeneration and functional recovery after complete spinal cord transection in rats by delayed treatment with transplants and neurotrophins. *J Neurosci* 2001;21:9334–9344. [PubMed: 11717367]
- Diamond ME, Huang W, Ebner FF. Laminar comparison of somatosensory cortical plasticity. *Science* 1994;265:1885–1888. [PubMed: 8091215]
- Diener PS, Bregman BS. Fetal spinal cord transplants support growth of supraspinal and segmental projections after cervical spinal cord hemisection in the neonatal rat. *J Neurosci* 1998a;18:779–793. [PubMed: 9425019]
- Diener PS, Bregman BS. Fetal spinal cord transplants support the development of target reaching and coordinated postural adjustments after neonatal cervical spinal cord injury. *J Neurosci* 1998b;18:763–778. [PubMed: 9425018]
- Dobkin BH, Havton LA. Basic advances and new avenues in therapy of spinal cord injury. *Annu Rev Med* 2004;55:255–282. [PubMed: 14746521]
- Dobrossy MD, Dunnett SB. Optimising plasticity: environmental and training associated factors in transplant-mediated brain repair. *Rev Neurosci* 2005;16:1–21. [PubMed: 15810651]
- Donoghue JP, Wise SP. The motor cortex of the rat: cytoarchitecture and microstimulation mapping. *J Comp Neurol* 1982;212:76–88. [PubMed: 6294151]
- Fernandes KJ, Fan DP, Tsui BJ, Cassar SL, Tetzlaff W. Influence of the axotomy to cell body distance in rat rubrospinal and spinal motoneurons: differential regulation of GAP-43, tubulins, and neurofilament-M. *J Comp Neurol* 1999;414:495–510. [PubMed: 10531542]
- Fiala JC, Feinberg M, Popov V, Harris KM. Synaptogenesis via dendritic filopodia in developing hippocampal area CA1. *J Neurosci* 1998;18:8900–8911. [PubMed: 9786995]
- Fifkova E, Anderson CL. Stimulation-induced changes in dimensions of stalks of dendritic spines in the dentate molecular layer. *Exp Neurol* 1981;74:621–627. [PubMed: 7297640]
- Globus A, Rosenzweig MR, Bennett EL, Diamond MC. Effects of differential experience on dendritic spine counts in rat cerebral cortex. *J Comp Physiol Psychol* 1973;82:175–181. [PubMed: 4571892]
- Hagg T. Collateral sprouting as a target for improved function after spinal cord injury. *J Neurotrauma* 2006;23:281–294. [PubMed: 16629616]
- Hayashi Y, Majewska AK. Dendritic spine geometry: functional implication and regulation. *Neuron* 2005;46:529–532. [PubMed: 15944122]
- Iarikov DE, Kim BG, Dai HN, McAtee M, Kuhn PL, Bregman BS. Delayed transplantation with exogenous neurotrophin administration enhances plasticity of corticofugal projections after spinal cord injury. *J Neurotrauma* 2007;24:690–702. [PubMed: 17439351]
- Jain N, Catania KC, Kaas JH. Deactivation and reactivation of somatosensory cortex after dorsal spinal cord injury. *Nature* 1997;386:495–498. [PubMed: 9087408]

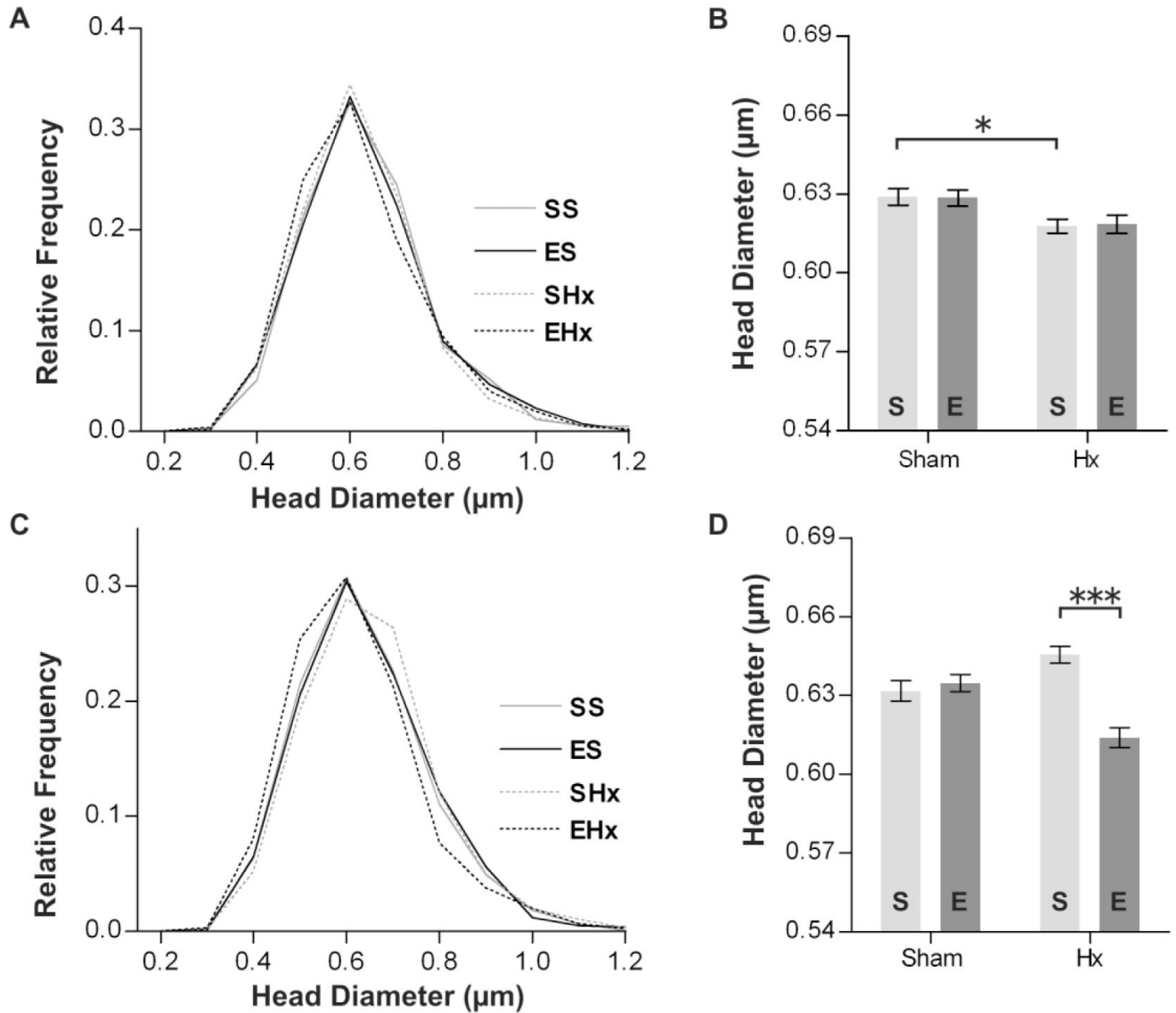
- Johansson BB, Belichenko PV. Neuronal plasticity and dendritic spines: effect of environmental enrichment on intact and postischemic rat brain. *J Cereb Blood Flow Metab* 2002;22:89–96. [PubMed: 11807398]
- Kasai H, Matsuzaki M, Noguchi J, Yasumatsu N, Nakahara H. Structure-stability-function relationships of dendritic spines. *Trends Neurosci* 2003;26:360–368. [PubMed: 12850432]
- Keene ON. The log transformation is special. *Stat Med* 1995;14:811–819. [PubMed: 7644861]
- Kim BG, Dai HN, McAtee M, Vicini S, Bregman BS. Remodeling of synaptic structures in the motor cortex following spinal cord injury. *Exp Neurol* 2006;198:401–415. [PubMed: 16443221]
- Kim BG, Dai HN, McAtee M, Vicini S, Bregman BS. Labeling of dendritic spines with the carbocyanine dye DiI for confocal microscopic imaging in lightly fixed cortical slices. *J Neurosci Methods* 2007;162:237–243. [PubMed: 17346799]
- Koch C, Zador A, Brown TH. Dendritic spines: convergence of theory and experiment. *Science* 1992;256:973–974. [PubMed: 1589781]
- Koopmans GC, Brans M, Gomez-Pinilla F, Duis S, Gispen WH, Torres-Aleman I, Joosten EA, Hamers FP. Circulating insulin-like growth factor I and functional recovery from spinal cord injury under enriched housing conditions. *Eur J Neurosci* 2006;23:1035–1046. [PubMed: 16519668]
- Lankhorst AJ, ter Laak MP, van Laar TJ, van Meeteren NL, de Groot JC, Schrama LH, Hamers FP, Gispen WH. Effects of enriched housing on functional recovery after spinal cord contusive injury in the adult rat. *J Neurotrauma* 2001;18:203–215. [PubMed: 11229712]
- Lendvai B, Stern EA, Chen B, Svoboda K. Experience-dependent plasticity of dendritic spines in the developing rat barrel cortex in vivo. *Nature* 2000;404:876–881. [PubMed: 10786794]
- Lynskey JV, Sandhu FA, Dai HN, McAtee M, Slotkin NR, Macarthur L, Bregman BS. Delayed intervention with transplants and neurotrophic factors supports recovery of forelimb function after cervical spinal cord injury in adult rats. *J Neurotrauma* 2006;23:617–634. [PubMed: 16689666]
- Marino RJ, Ditunno JF Jr, Donovan WH, Maynard F Jr. Neurologic recovery after traumatic spinal cord injury: data from the Model Spinal Cord Injury Systems. *Arch Phys Med Rehabil* 1999;80:1391–1396. [PubMed: 10569432]
- Martinez A, Alcantara S, Borrell V, Del Rio JA, Blasi J, Otal R, Campos N, Boronat A, Barbacid M, Silos-Santiago I, Soriano E. TrkB and TrkC signaling are required for maturation and synaptogenesis of hippocampal connections. *J Neurosci* 1998;18:7336–7350. [PubMed: 9736654]
- Matsuzaki M, Honkura N, Ellis-Davies GC, Kasai H. Structural basis of long-term potentiation in single dendritic spines. *Nature* 2004;429:761–766. [PubMed: 15190253]
- McKinley PA, Jenkins WM, Smith JL, Merzenich MM. Age-dependent capacity for somatosensory cortex reorganization in chronic spinal cats. *Brain Res* 1987;428:136–139. [PubMed: 3815108]
- Miller M, Peters A. Maturation of rat visual cortex. II. A combined Golgi-electron microscope study of pyramidal neurons. *J Comp Neurol* 1981;203:555–573. [PubMed: 7035504]
- Miya D, Giszter S, Mori F, Adipudi V, Tessler A, Murray M. Fetal transplants alter the development of function after spinal cord transection in newborn rats. *J Neurosci* 1997;17:4856–4872. [PubMed: 9169544]
- Moser MB, Trommald M, Andersen P. An increase in dendritic spine density on hippocampal CA1 pyramidal cells following spatial learning in adult rats suggests the formation of new synapses. *Proc Natl Acad Sci U S A* 1994;91:12673–12675. [PubMed: 7809099]
- Nikulina E, Tidwell JL, Dai HN, Bregman BS, Filbin MT. The phosphodiesterase inhibitor rolipram delivered after a spinal cord lesion promotes axonal regeneration and functional recovery. *Proc Natl Acad Sci U S A* 2004;101:8786–8790. [PubMed: 15173585]
- Nimchinsky EA, Oberlander AM, Svoboda K. Abnormal development of dendritic spines in FMR1 knock-out mice. *J Neurosci* 2001;21:5139–5146. [PubMed: 11438589]
- Noguchi J, Matsuzaki M, Ellis-Davies GC, Kasai H. Spine-neck geometry determines NMDA receptor-dependent  $Ca^{2+}$  signaling in dendrites. *Neuron* 2005;46:609–622. [PubMed: 15944129]
- Ohlsson AL, Johansson BB. Environment influences functional outcome of cerebral infarction in rats. *Stroke* 1995;26:644–649. [PubMed: 7709412]
- Portera-Cailliau C, Pan DT, Yuste R. Activity-regulated dynamic behavior of early dendritic protrusions: evidence for different types of dendritic filopodia. *J Neurosci* 2003;23:7129–7142. [PubMed: 12904473]

- Purpura DP. Dendritic differentiation in human cerebral cortex: normal and aberrant developmental patterns. *Adv Neurol* 1975;12:91–134. [PubMed: 1155280]
- Raineteau O, Schwab ME. Plasticity of motor systems after incomplete spinal cord injury. *Nat Rev Neurosci* 2001;2:263–273. [PubMed: 11283749]
- Restivo L, Ferrari F, Passino E, Sgobio C, Bock J, Bagni C, Ammassari-Teule M. Enriched environment promotes behavioral and morphological recovery in a mouse model for the fragile X syndrome. *Proc Natl Acad Sci U S A* 2005;102:11557–11562. [PubMed: 16076950]
- Segal M. Dendritic spines and long-term plasticity. *Nat Rev Neurosci* 2005;6:277–284. [PubMed: 15803159]
- Sheng M, Kim MJ. Postsynaptic signaling and plasticity mechanisms. *Science* 2002;298:776–780. [PubMed: 12399578]
- Svoboda K, Tank DW, Denk W. Direct measurement of coupling between dendritic spines and shafts. *Science* 1996;272:716–719. [PubMed: 8614831]
- Topka H, Cohen LG, Cole RA, Hallett M. Reorganization of corticospinal pathways following spinal cord injury. *Neurology* 1991;41:1276–1283. [PubMed: 1866018]
- Van Meeteren NL, Eggers R, Lankhorst AJ, Gispens WH, Hamers FP. Locomotor recovery after spinal cord contusion injury in rats is improved by spontaneous exercise. *J Neurotrauma* 2003;20:1029–1037. [PubMed: 14588119]
- Wallace W, Bear MF. A morphological correlate of synaptic scaling in visual cortex. *J Neurosci* 2004;24:6928–6938. [PubMed: 15295028]
- Yuste R, Bonhoeffer T. Morphological changes in dendritic spines associated with long-term synaptic plasticity. *Annu Rev Neurosci* 2001;24:1071–1089. [PubMed: 11520928]
- Yuste R, Majewska A, Holthoff K. From form to function: calcium compartmentalization in dendritic spines. *Nat Neurosci* 2000;3:653–659. [PubMed: 10862697]

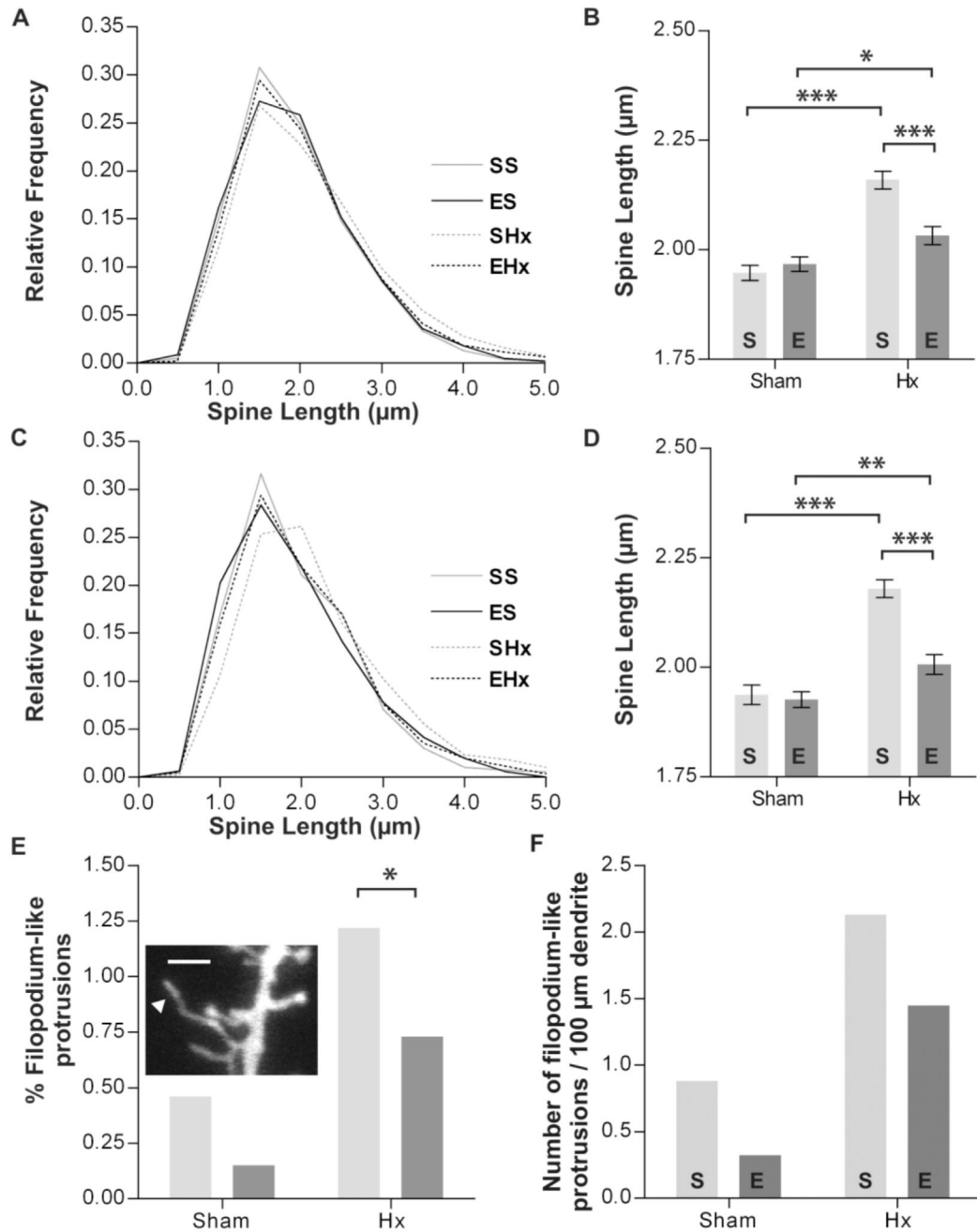


**Fig. 1.** Effects of enriched housing and spinal cord injury on spine density in the motor cortex. **A:** Representative images of dendritic segments in the superficial layer. Each image is a 3D projection consisting of stack images with different optical sections (step size 0.4 – 0.6 μm). **B,C:** Spine density data from basal dendrites in the superficial layer (layers 2/3). **B:** Cumulative frequency histogram of spine density. **C:** Comparison of mean spine density from the same set of data. Light and dark gray bars represent mean spine density  $\pm$  SEM of the groups in standard (S) and enriched (E) housing conditions, respectively. Injury conditions are indicated as sham or Hx (hemisection injury). **D,E:** Spine density data from basal dendrites in the deep layer (layers 5/6). **D:** Cumulative frequency histogram of spine density. **E:** Comparison of mean

spine density from the same set of data. Light and dark gray bars represent mean spine density  $\pm$  SEM of the groups in standard (S) and enriched (E) housing conditions, respectively. Injury conditions are indicated as sham or Hx.  $*P < 0.05$  and  $***P < 0.001$  by two-way ANOVA, followed by post hoc Bonferroni's test. For the number of dendritic segments analyzed in each group see Table 1 and 2. SS, sham controls in standard housing; ES, sham controls in enriched housing; SHx, injured animals in standard housing; EHx, injured animals in enriched housing. Scale bar = 2  $\mu$ m.

**Fig. 2.**

Effects of enriched housing and spinal cord injury on spine head diameter in the motor cortex. A,B: Head diameter of dendritic spines from the dendritic segments in the superficial layer (layers 2/3). **A:** Frequency histogram of head diameter. **B:** Comparison of mean head diameter from the same set of data. Light and dark gray bars represent mean head diameter  $\pm$  SEM of the groups in standard (S) and enriched (E) housing conditions, respectively. Injury conditions are indicated as sham or Hx (hemisection injury). C,D: Head diameter of dendritic spines from the dendritic segments in the deep layers (layer 5/6). **C:** Frequency histogram of head diameter. **D:** Comparison of mean head diameter from the same set of data. Light and dark gray bars represent mean head diameter  $\pm$  SEM of the groups in standard (S) and enriched (E) housing conditions, respectively. Injury conditions are indicated as sham or Hx. \* $P < 0.05$  and \*\*\* $P < 0.001$  by two-way ANOVA, followed by post hoc Bonferroni's test. For the number of dendritic spines analyzed in each group see Tables 1 and 2. SS, sham controls in standard housing; ES, sham controls in enriched housing; SHx, injured animals in standard housing; EHx, injured animals in enriched housing.

**Fig. 3.**

Effects of enriched housing and spinal cord injury on the length of dendritic spines in the motor cortex. **A,B:** Length of dendritic spines from the dendritic segments in the superficial layer (layers 2/3). **A:** Frequency histogram of spine length. **B:** Comparison of mean spine length from the same set of data. Light and dark gray bars represent mean spine length  $\pm$  SEM of the groups in standard (S) and enriched (E) housing conditions, respectively. Injury conditions are indicated as sham or Hx (hemisection injury). **C,D:** Length of dendritic spines from the dendritic segments in the deep layer (layers 5/6). **C:** Frequency histogram of spine length. **D:** Comparison of mean spine length from the same set of data. Light and dark gray bars represent mean spine length  $\pm$  SEM of the groups in standard (S) and enriched (E) housing conditions,

respectively. Injury conditions are indicated as sham or Hx.  $*P < 0.05$ ,  $**P < 0.01$ , and  $***P < 0.001$  by two-way ANOVA, followed by post hoc Bonferroni's test. For the number of dendritic spines analyzed in each group see Tables 1 and 2. **E**: Comparison of the frequency of filopodium-like long protrusions between the experimental groups. Light and dark gray bars represent percentage of the total number of spines analyzed in each group in standard (S) and enriched (E) housing conditions, respectively.  $*P < 0.05$  by  $\chi^2$  analysis. **Inset**: Example of filopodium-like dendritic protrusion (arrowhead). Scale bar = 2  $\mu\text{m}$ . **F**: Comparison of the mean number of filopodium-like long protrusions per 100  $\mu\text{m}$  dendrite. SS, sham controls in standard housing; ES, sham controls in enriched housing; SHx, injured animals in standard housing; EHx, injured animals in enriched housing.

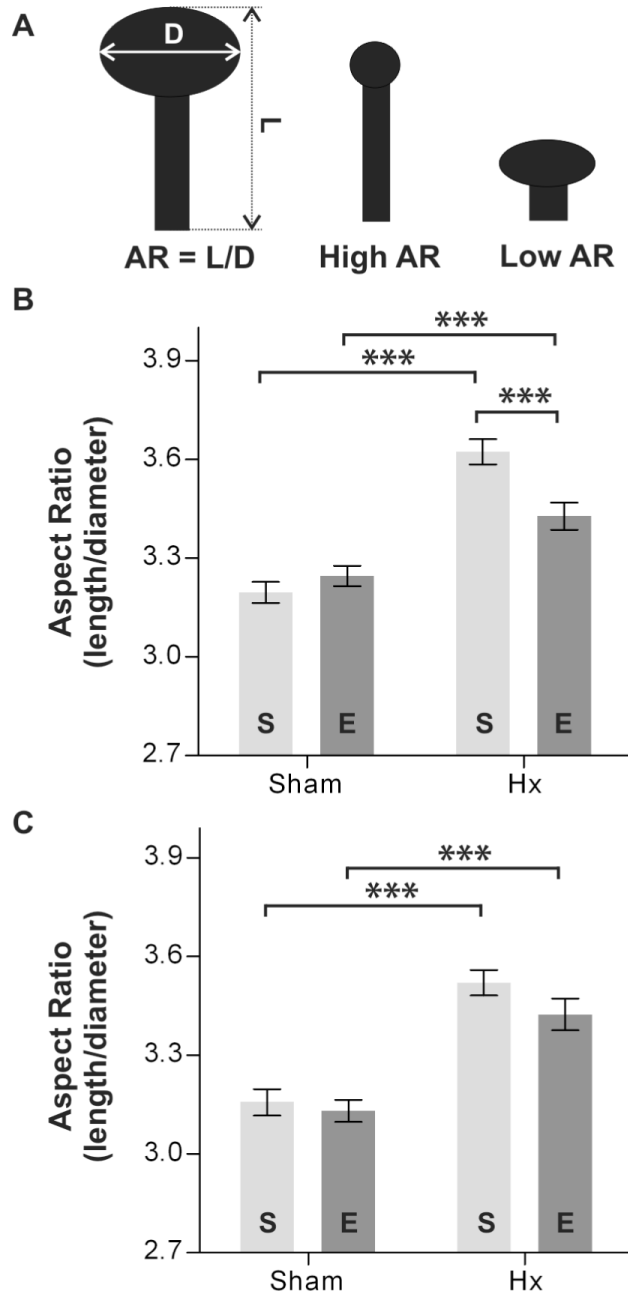


**Fig. 4.** Effects of enriched housing and spinal cord injury on the aspect ratio of dendritic spines in the motor cortex. **A:** Aspect ratio (AR) was defined as the value of spine length (L) divided by that of head diameter (D) from each spine. The higher the AR, the more slender or elongated the spine morphology. The lower the AR, in contrast, the shorter or fatter the spine morphology. **B,C:** The mean AR as a function of different housing and injury conditions in the superficial (layers 2/3) and deep layer (layers 5/6), respectively. Gray and black bars represent mean AR  $\pm$  SEM of the groups in standard (S) and enriched (E) housing conditions, respectively. Injury conditions are indicated as sham or Hx (hemisection injury). \*\*\* $P < 0.001$  by two-way

ANOVA, followed by post hoc Bonferroni's test. For the number of dendritic spines analyzed in each group see Tables 1 and 2.

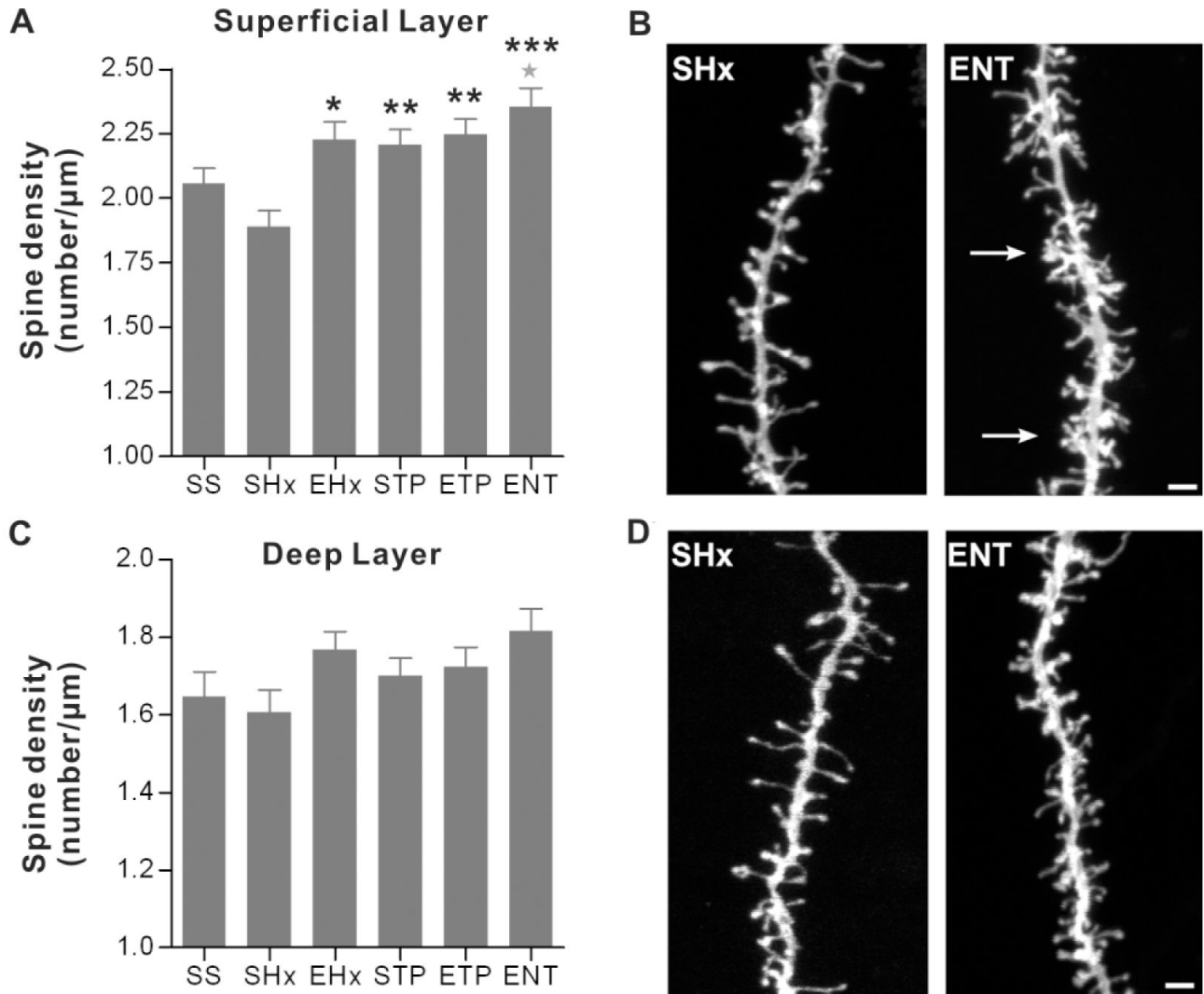


**Fig. 5.** Changes in spine density in the motor cortex after spinal cord injury and different combinations of interventions. **A,C:** Spine density data from basal dendrites in the superficial (layers 2/3) and deep (layers 5/6) layers. Error bars represent SEM. \* $P < 0.05$  compared with SS group; \*\* $P < 0.01$ , \*\*\* $P < 0.001$  compared with SHx group by one-way ANOVA, followed by post hoc Bonferroni's test. For the number of dendritic segments analyzed in each group see Tables 1 and 2. SS, sham controls in standard housing; SHx, injured animals in standard housing; EHx, injured animals in enriched housing; STP, injured animals in standard housing that received transplantation; ETP, injured animals in enriched housing that received transplantation; ENT, injured animals in enriched housing that received transplantation plus NT-3. **B,D:** Representative images of dendritic segments in SHx and ENT group in the superficial and deep layers, respectively. In some of the superficial layer dendritic segments in NT-3 group, spines were too crowded to delineate individual spines even with scrolling through a series of stack images with different optical section (arrows). Scale bar = 2  $\mu\text{m}$ .

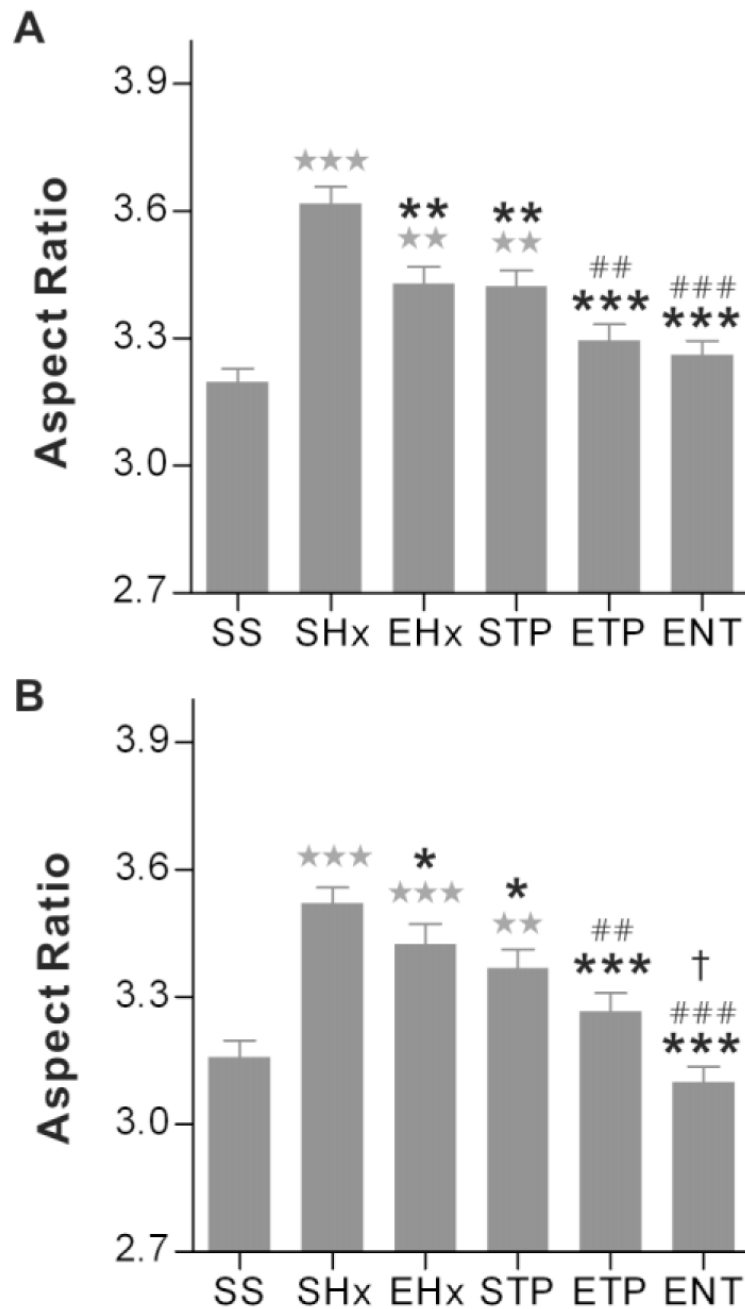


**Fig. 6.** Changes in the aspect ratio of dendritic spines in the motor cortex after spinal cord injury and different combinations of interventions. **A,B:** Aspect ratio (AR) data from basal dendrites in the superficial (layers 2/3) and deep (layers 5/6) layers, respectively. AR was defined as the value of spine length divided by that of head diameter from each spine. Error bars represent SEM. \*\* $P < 0.01$ , \*\*\* $P < 0.001$  compared with SS group; \* $P < 0.05$ , \*\* $P < 0.01$ , and \*\*\* $P < 0.001$  compared with SHx group; ## $P < 0.01$ , ### $P < 0.01$  compared with EHx group; † $P < 0.05$  compared with ETP group by Kruskal-Wallis test followed by post hoc Mann-Whitney U test. For the number of dendritic spines analyzed in each group see Tables 1 and 2. SS, sham controls in standard housing; SHx, injured animals in standard housing; EHx,

injured animals in enriched housing; STP, injured animals in standard housing that received transplantation; ETP, injured animals in enriched housing that received transplantation; ENT, injured animals in enriched housing that received transplantation plus NT-3.

**TABLE 1**  
Summary of the Measured Variables from Dendritic Spines in the Superficial Layer<sup>1</sup>

	SS	ES	SHx	EHx	STP	ETP	ENT
No. of animals	5	6	6	6	5	5	5
No. of dendritic segments	32	34	37	26	36	30	38
Average/total length of dendrites analyzed (µm)	27.3/872.1	26.2/890.6	30.5/1127.6	27.6/717.0	25.9/933.0	26.2/786.3	26.5/1007.4
No. of spines	1,777	2,041	2,140	1,589	2,057	1,765	2,368
Spine density (number/µm)							
Mean	2.06	2.29	1.91	2.23	2.21	2.25	2.35
Median	2.05	2.33	1.84	2.14	2.23	2.29	2.43
Coefficient of variation (%)	16.8	15.3	18.2	15.5	16.3	14.5	19.0
Head diameter (µm)							
Mean	0.629	0.628	0.618	0.618	0.621	0.619	0.626
Median	0.610	0.606	0.606	0.602	0.606	0.602	0.606
Coefficient of variation (%)	21.3	22.1	20.3	22.8	23.6	25.2	23.8
Spine length (µm)							
Mean	1.95	1.97	2.16	2.03	2.03	1.96	1.96
Median	1.82	1.87	1.96	1.88	1.92	1.77	1.82
Coefficient of variation (%)	37.7	37.9	42.5	40.6	39.1	42.6	39.5
Aspect ratio							
Mean	3.20	3.25	3.62	3.43	3.42	3.29	3.26
Median	2.92	2.95	3.21	3.04	3.07	2.97	2.93
Coefficient of variation (%)	41.6	43.0	48.9	48.1	47.7	47.6	46.9

<sup>1</sup> SS, sham controls in standard housing; ES, sham controls in enriched housing; SHx, injured animals in standard housing; EHx, injured animals in enriched housing; STP, injured animals in standard housing that received transplantation; ETP, injured animals in enriched housing that received transplantation; ENT, injured animals in enriched housing that received transplantation plus NT-3.

TABLE 2

Summary of the Measured Variables in the Deep Layer<sup>1</sup>

	SS	ES	SHx	EHx	STP	ETP	ENT
No. of animals	5	6	6	6	5	5	5
No. of dendritic segments	27	38	38	29	33	30	35
Average/total length of dendrites analyzed (µm)	28.6/771.8	26.7/1013.0	32.1/1217.9	27.7/802.2	27.4/902.6	27.2/815.5	27.0/944.9
No. of spines	1,261	1,865	1,947	1,412	1,529	1,400	1,701
Spine density (number/µm)							
Mean	1.65	1.85	1.61	1.77	1.70	1.72	1.82
Median	1.54	1.83	1.50	1.79	1.73	1.71	1.83
Coefficient of variation (%)	20.6	20.4	22.6	23.1	22.1	23.1	22.8
Head diameter (µm)							
Mean	0.632	0.635	0.646	0.614	0.632	0.631	0.633
Median	0.610	0.610	0.634	0.602	0.610	0.610	0.610
Coefficient of variation (%)	22.0	22.5	21.8	22.8	23.6	25.2	23.8
Spine length (µm)							
Mean	1.94	1.93	2.18	2.01	2.04	1.97	1.88
Median	1.77	1.78	1.99	1.84	1.91	1.79	1.76
Coefficient of variation (%)	40.9	41.1	40.7	42.3	40.7	42.5	38.1
Aspect ratio							
Mean	3.16	3.13	3.52	3.42	3.37	3.27	3.10
Median	2.87	2.79	3.15	3.03	3.00	2.86	2.79
Coefficient of variation (%)	44.8	44.9	48.5	52.5	49.8	50.7	46.9

<sup>1</sup> SS, sham controls in standard housing; ES, sham controls in enriched housing; SHx, injured animals in standard housing; EHx, injured animals in enriched housing; STP, injured animals in standard housing that received transplantation; ETP, injured animals in enriched housing that received transplantation; ENT, injured animals in enriched housing that received transplantation plus NT-3.